

Associations of decimetric type III bursts with coronal mass ejections and H α flares *

Yuan Ma¹, De-Yu Wang², Jun Lin^{1,3}, Shuo Dai¹ and Xue-Fei Zhang¹

¹ National Astronomical Observatories of China / Yunnan Astronomical Observatory, Chinese Academy of Sciences, Kunming 650011, China

² Purple Mountain Observatory, Chinese Academy of Sciences, Nanjing 210008, China

³ Harvard-Smithsonian Center for Astrophysics, Cambridge, MA 02138, USA; jlin@ynao.ac.cn

Received 2009 October 1; accepted 2010 February 22

Abstract We present a statistical study of decimetric type III radio bursts, coronal mass ejections (CMEs), and H α flares observed in the period from July 2000 to March 2005. In total, we investigated 395 decimetric type III radio burst events, 21% of which showed apparent correlation to CMEs that were associated with H α flares. We noticed that the H α flares which were strongly associated with CMEs were gradual events, and 82% of them took place before CMEs appeared in the field of view of LASCO C2; that most of the CME-associated radio bursts started in the frequency range around 750 MHz with a frequency drifting rate of several hundred MHz s⁻¹, of which both positive and negative ones were recognized; and that the correlation of type III radio bursts to CMEs without associated flares is fairly vague, less than 9%.

Key words: Sun: magnetic fields — Sun: flares — Sun: radio bursts — Sun: coronal mass ejections

1 INTRODUCTION

It is now well accepted that solar eruption results from the rapid release of magnetic energy previously stored in the solar corona, and generates various phenomena, including solar flares, eruptive prominences, and coronal mass ejections (CMEs). Associated with these phenomena is the continuum electromagnetic emission that spans the dynamic range from radio to microwaves, visible light, soft and hard X-rays, γ -rays, and so on. The emission in the radio band offers several important diagnostic tools to address long-standing questions about energy release, plasma heating, particle acceleration, and particle transportation in magnetized plasmas. Therefore, these various manifestations should show certain correlations with one another.

Usually, type III radio bursts often take place which are strongly associated with hard X-ray emissions and H α flares, and are also accompanied with other radio bursts at microwave frequencies (e.g., see Švestka 1976; Bastian et al. 1998; Yan et al. 2006; and references therein). The type III burst is the plasma radiation excited by energetic electron beams propagating along the magnetic field lines toward and away from the Sun, and appears in a dynamic spectrum as almost vertical features because of the high frequency drifting rate. More detailed discussions on type III bursts

* Supported by the National Natural Science Foundation of China.

can be found in works by Ginzburg & Zhelezniakov (1958), Chernov (1997), Dulk et al. (2000), and Gopalswamy (2004, and references therein). Direct observations of nonthermal electrons and plasma waves in space, in association with type III bursts, provided solid evidence for the plasma emission mechanism (Lin & Anderson 1973).

Commonly, the type III radio bursts with positive drifting rate, produced by the electron beams propagating towards the Sun, are closely related to other activities. For example, Aschwanden (2002) showed that 48% of positive drift decimetric type III radio bursts are correlated with HXR bursts, and Bastian et al. (1998) pointed out that the number of type III bursts in the decimetric wave band in a flare can be as high as several hundred, and often exceeds the number of HXR peaks by an order of magnitude.

As one of the manifestations of a solar eruption, CMEs should necessarily display a correlation to the radio bursts. However, such correlations, especially that of CMEs to type III radio bursts in the decimetric wavelength, have not received enough attention, although there have been a couple of works on this issue performed recently (Reiner et al. 2000 and 2008). Studying such a correlation may provide us with useful information for better understanding the physics of the energy conversion in the eruption, including magnetic reconnection and its consequences (e.g., see Maia et al. 1998; Reiner et al. 2000 as well as discussions of Cecatto et al. 2004).

Jackson et al. (1978) suggested that the pre-transient shock wave and the type III radio burst might be used as an indicator of CMEs. Michalek & Zaczkowski (2002) analyzed the relation of type III bursts to CMEs, and pointed out that the difference between the starting time of CMEs and that of radio bursts should strongly depend on the CME positions on the Sun (e.g., see also Munro et al. 1979). So from observations of type III radio bursts and the CME-flare-radio burst relationship, we may be able to estimate the time of CME initiation, and to locate the source region of the radio bursts.

Previous studies of the association of CMEs to type III radio bursts have yielded several important results (Jackson et al. 1978; Maia et al. 1998; Reiner et al. 2000, 2008; Michalek et al. 2001; Cane et al. 2002; Michalek & Zaczkowski 2002; Cecatto et al. 2004; Yan et al. 2006), and theoretical work by Lin et al. (2006) also began to pursue the physics behind the observed association, but it is not quite clear how well the small scale decimetric type III bursts could correlate to the large scale CMEs. To look into this issue in detail, we perform a statistical study of the type III radio bursts observed by the 625–1500 MHz radio spectrograph of the Yunnan Astronomical Observatory (YNAO), China, and investigate the related correlations in which both CMEs and H α flares are involved.

We will briefly introduce the instruments and observational data used in this work in the next section, deduce and analyze these data in Section 3, and discuss our results and summarize this work in Section 4.

2 INSTRUMENTATION AND OBSERVATIONS

The data of the type III radio bursts used in this work were taken by the radio spectrograph of YNAO. The working frequencies of the instrument range from 625 to 1500 MHz, with a time resolution of 8 ms and a frequency resolution of 1.37 MHz. The diameter of the antenna is 10 m. Since the instrument started operation in July 2000, a lot of radio burst events have been recorded and 395 type III bursts which are among them, together with the associated CMEs and flares, have been studied. The information on H α flares is from the Solar Geophysics Data (SGD) and the Chinese Solar Geophysics Data (CSGD), while the data for the associated CMEs are from the SOHO/LASCO/C2 CME catalog. The full disk H α images in the spectral line center were from both YNAO and the Kanzelhoeke Solar Observatory (KSO), Austria. Two criteria for identifying type III radio bursts are used: the duration of each single signal's half-power is less than 2.5 ms; and the corresponding frequency drifting rate is less than 10 GHz s⁻¹.

3 ASSOCIATIONS OF TYPE III RADIO BURSTS TO CMES AND H α FLARES

If we just consider the time correlation of the type III bursts to CMES and flares only, among the 395 radio bursts observed by the radio spectrograph of YNAO, 187 (about 47%) events were associated with CMES, and 150 (38%) were associated with H α flares. Overlap of these two groups of radio burst events exists, and only 36 (9%) radio burst events were associated with CMES alone. In fact, the type III radio bursts associated with CMES alone were rarely observed, and the correlation of 9% obtained here was deduced without considering whether source regions of CMES and radio burst sources were co-located in space. Considering the factor of locations brings the correlation to zero.

Since the radio spectrograph does not have spatial resolution, on the other hand, we are not able to identify the location where the radio bursts directly came from. So it is very likely to yield incorrect conclusions for the CME-type III burst correlation if time is the only issue considered for the correlation. Therefore, we need to investigate the behaviors of type III radio bursts and the possible associated CMES in both time and space, especially the source regions of CMES.

We select and analyze the data, and identify the events in the following way: we start with collecting the data of the type III radio bursts associated with H α flares because both observations and theories indicate a good correlation of type III bursts to H α flares (e.g., Švestka 1976; Klassen et al. 2003; Lin et al. 2006; and references therein); then the events of type III bursts associated with both flares and CMES are identified and selected. The onset time and position of H α flares can be found in SGD, and the time when a CME first appears in the FOV of LASCO/C2 is taken from both the SOHO/LASCO/C2 CME catalog¹ and the Preliminary 2003 SOHO LASCO Coronal Mass Ejection List².

Here we choose two events, as examples, to demonstrate how we correlate flares, CMES, and decimetric type III radio bursts to one another. The first event occurred in active region AR 9906 on 2002 April 17 that generated type III radio bursts with a negative frequency drifting rate, and the second one took place in AR 10696 on 2004 November 10 that generated radio bursts with a positive frequency drifting rate. Figures 1 and 2 display these two events observed in different wavelengths.

The first event developed an M2.6/2N flare (Fig. 1(a)) and a halo CME (Fig. 1(b)) with a speed of 1200 km s⁻¹ (a fast CME), and produced two groups of type III radio bursts in the decimetric frequency range from 720 to 790 MHz (Fig. 2(a)). Figure 1(a) displays an H α filtergram of the flare from YNAO taken at 08:20:17 UT, and Figure 1(b) is a composite of two running difference images from EIT 195 Å for the flare and LASCO/C2 (for CME), respectively. The CME first appeared in the FOV of LASCO/C2 in the time interval between 08:06 and 08:26 UT. The flare observed in EIT 195 Å is circled in Figure 1(b). Comparison of these two figures and relevant details of the flare and the CME simply suggest the correlation of the CME to the flare.

To establish the correlation of the flare, CME, and radio burst to one another, we now carefully determine the initial time of the first group of radio bursts. Figure 2(a) plots the variations of the radio burst signal strength versus time for different frequencies. From these curves, we can tell that the first radio burst signal appeared at about 07:49:28 UT, and the drifting rates of these two groups of bursts were -375 and -68 MHz s⁻¹, respectively. Then we look for the activities observed in different wavelengths occurring around the same time. We recognized that an M2.6/2N flare (Fig. 1(a)) in AR 9906 commenced at 07:50 UT, and reached its maximum at 08:15 UT. Meanwhile, we do not find any other activity outside AR 9906 taking place at this time. This, together with the close occurrences of the flare and the radio burst in time, constitutes the correlation of the M2.6/2N flare to the decimetric type III radio burst (see Fig. 2(a) as well). Considering the correlation of the CME to the flare which developed in a short amount of time, we thus establish the correlation of the M2.6/2N flare, the fast CME, and the decimetric radio burst to one another for the 2002 April 17 event.

¹ http://cdaw.gsfc.nasa.gov/CME_list/

² ftp://lasco6.nascom.nasa.gov/pub/lasco/status/LASCO_CME_List_2003

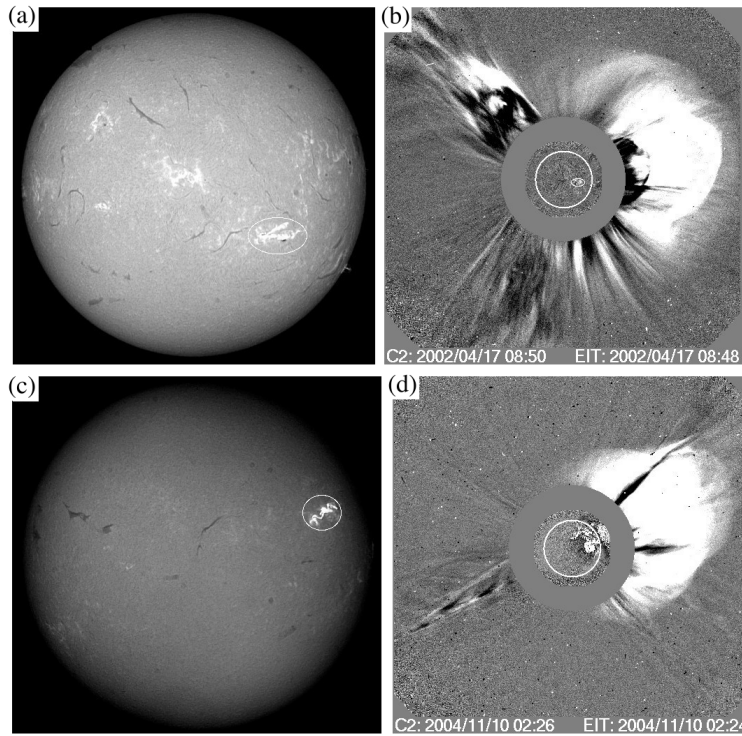


Fig. 1 2002 April 17 event (panels a and b) and the 2004 November 10 event (panels c and d) observed in various wavelengths by different instruments. (a, c) The H α filtergram of the full disk image of the Sun observed by YNAO; the flare region is circled by a white oval; (b, d) the composite of an EIT 195 running difference image and a LASCO/C2 running difference image, with a white oval which roughly surrounds the flare region in panel (b).

The second event took place in AR 10696 at N09W49 on 2004 November 10. It produced an X2.5/3B flare (Fig. 1(c)), and a very fast CME ($\sim 3400 \text{ km s}^{-1}$, seen in the field of view [FOV] of LASCO/C2, Fig. 1(d)), and several groups of type III radio bursts are in the frequency range from 1128 to 1205 MHz (Fig. 2(b)). In this event, the H α flare (Fig. 1(c)) was observed to start at 02:04 UT, roughly 5 minutes before the radio burst appeared for the first time, and reached its maximum at 02:10 UT.

Figure 1(d) is a composite of an EIT 195 Å running difference image and a LASCO/C2 running difference image, and Figure 2(b) indicates that the apparent type III burst first commenced slightly earlier than 02:09:03 UT from a frequency of 1.13 GHz; the peak of the radio emission drifted from low to high frequencies at a rate of about 440 MHz s^{-1} . The associated CME was a halo one and entered the FOV of LASCO/C2 some time between 02:06 and 02:26 UT. As we did for the first event, comparison of the H α image (Fig. 1(c)) and the LASCO/C2 and EIT composite (Fig. 1(d)) suggests the correlation of the H α flare to the CME observed in this event.

We further went through the eruption information given by SGD, and noticed that the eruption occurring in AR 10720 was the sole event taking place at around 02:09 UT. This indicates that the type III radio burst was related to the H α flare happening in AR 10720, and therefore the correlation of the three manifestations to one another is established. Following the same practice, we are able to

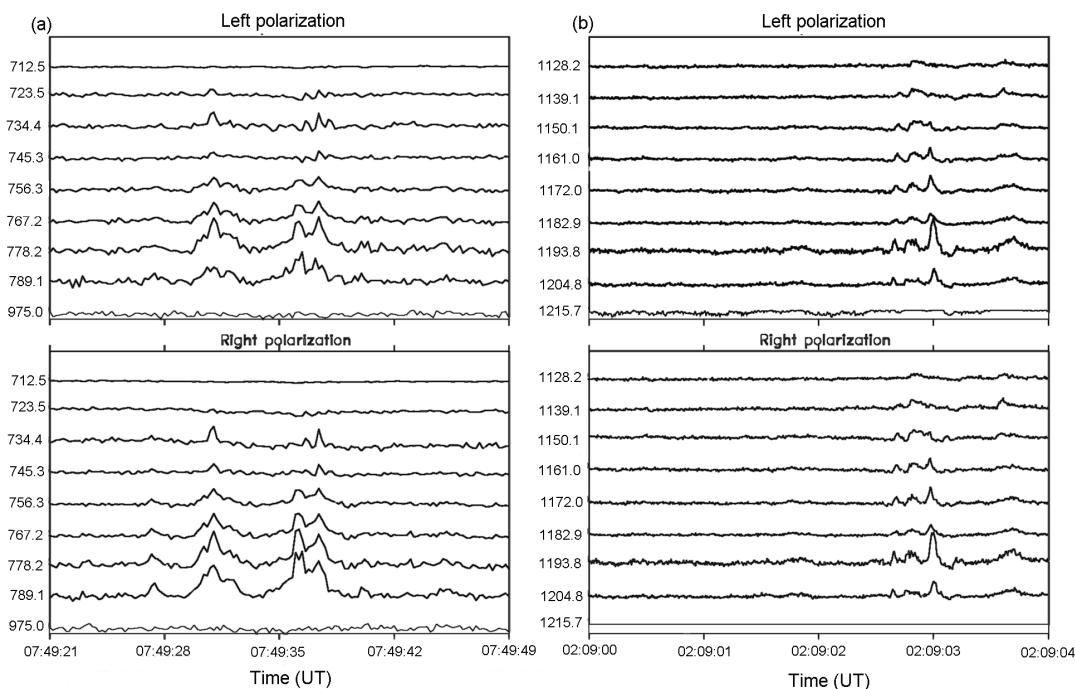


Fig. 2 (a) Dynamic spectra of the 2002 April 17 event covering the frequency range from 720 to 790 MHz, and two groups of the burst show frequency drifting rates of -375 and -68 MHz s^{-1} , respectively; and (b) that of the 2004 November 10 event covering the frequency range from 1128 to 1205 MHz, in which the signal manifests a frequency drifting rate of around 440 MHz s^{-1} .

investigate the possible relationship among $H\alpha$ flares, CMEs, and type III radio bursts in decimetric wavelengths observed in the events of interest, and to determine whether a corresponding correlation exists.

In this approach, on the other hand, determining CME positions on the solar surface accurately is an essential issue for correctly correlating the three objects: flares, CMEs and type III radio bursts, to one another. The time of CMEs discussed here is when CMEs first appeared in the field of view of LASCO C2. Obviously, this time is different from the CME onset time, which is usually defined in observations as when the CME or the eruptive prominence starts to take off, or as that theoretically predicted time when the disrupting magnetic configuration starts to lose its equilibrium (e.g., see Lin 2004).

Using this time to identify the CME may affect the accuracy and reliability of the correlation because it is very likely that two processes which do not have any physical connection may occur at the same time but at different locations. To avoid such mis-correlations, and as additional criteria in performing correlations, we double-checked the positions of both $H\alpha$ flares and CMEs, and excluded the cases in which the time difference between the occurrence of $H\alpha$ flares and that of radio bursts was longer than an hour. In doing so, we obtained the spatial resolution of a quarter of the solar disk for the radio burst, and significantly reduced the possibility of mis-correlations according to the conclusions of Lin et al. (2006) about type III bursts and flares. After all, it is hard for two events without any physical connection to take place successively within an hour in the same quarter of the

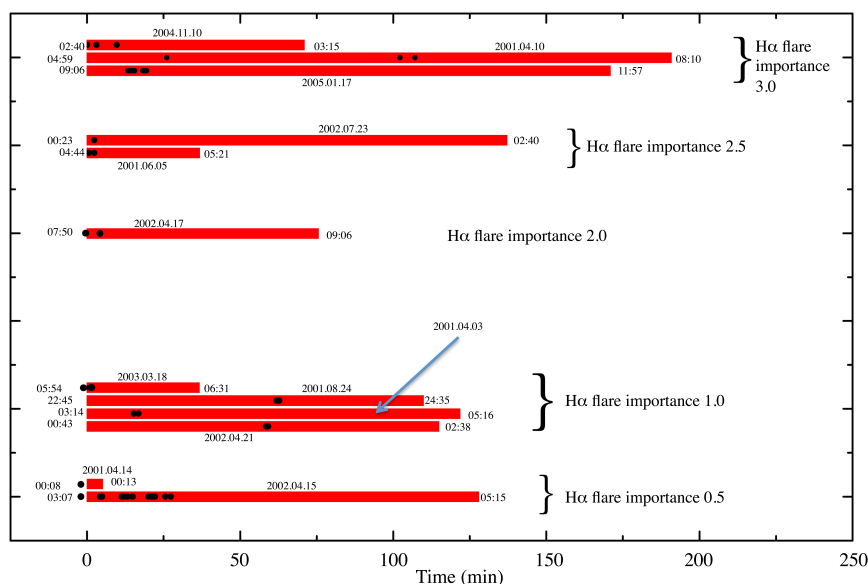


Fig. 3 Relative and true times of each H α flare and the associated type III radio bursts studied in the present work. The abscissa gives the period of H α flares with time zero being the onset time of each flare. Each horizontal stripe is for an H α flare, its left end is located at time zero, and the corresponding real time in UT is specified at the left. The time when the flare finished is given as well at the right, and the corresponding date of each flare is indicated above or below the stripe. All the flares are classified according to their H α importance into five groups, and those of the same importance are arranged in the same group with the flare importance being addressed at the right. Those black closed circles are for the radio bursts associated with the H α flares.

disk. Recently, Wang et al. (2006) found that the onset of a major event could impact an event a half disk away.

In addition, we also used the composite of running difference images of EIT 195 and LASCO/C2 to help identify the relationship between H α flares and CMEs. This further improves the accuracy of co-locating the source regions of radio bursts and CMEs to the associated H α flares. We understand that the poor spatial resolution of the radio data may still cause some uncertainties in our final results. However, to our knowledge, a method better than that which we have applied here to correlating CMEs, flares, and decimetric type III radio bursts to one another has not yet been reported.

Through the above approach, we found that there were 84 out of 395 (21%) events which displayed correlations of the type III radio bursts to both flares and CMEs. The value of this fraction is apparently smaller than the values ranging from 60% to 80%, which are for the events showing correlations of CMEs to type II radio bursts (e.g., see Munro et al. 1979; Sheeley et al. 1984; Shanmugaraju et al. 2003; Ma 2005).

To further confirm the relation of these radio bursts to both flares and CMEs studied in this work, we investigate the difference in times when the H α flares and the radio bursts commenced. We create a panel as shown in Figure 3. In this panel, the abscissa gives the period of H α flares with time zero being the onset time of each flare. Each horizontal stripe is for an H α flare, its left end is located at time zero, and the corresponding real time in UT is specified near the end in the form of 'hour:minute' in black. The time when the flare finished is given in UT as well near the right end of the stripe, and the corresponding date of each flare is indicated in the form of 'year.month.day'

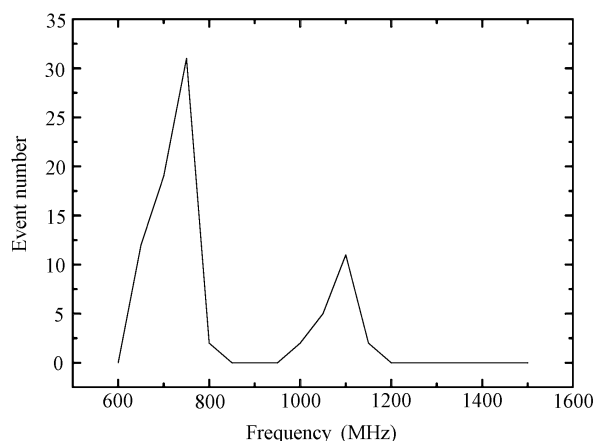


Fig. 4 Number of events versus the corresponding start frequencies of type III radio bursts.

above or below the stripe. All the flares are classified according to their $H\alpha$ importance into five groups, and those of the same importance are arranged in the same group with the flare importance being addressed at the right. Those black closed circles are for the radio bursts detected before or during the associated $H\alpha$ flares.

Usually, several groups of type III radio bursts are detected during a single flare, implying successive particle accelerations in the same flare process. So a black circle represents the burst that was detected first in each group, and is located at the time that the first burst was detected. From the panel, we notice that most (32 out of 36 groups) of the type III radio bursts we collected took place after the associated flares, but only a small part of them (4 out of 36) began prior to the flare. We also find that the onset times of 33 out of 36 groups of radio bursts differed from those of the associated flares by less than an hour, and only three of them commenced more than an hour after the flare. Therefore, the information revealed by the panel in Figure 3 indeed helps confirm the correlation of the radio bursts detected by the radio spectrograph at YNAO to the flares, as well as CMEs observed by other ground-based and space-born instruments.

This suggests that the three different manifestations, type III radio bursts, $H\alpha$ flares, and CMEs, studied in the present work are all products of the same energy conversion process in the solar eruption. The related details of such correlations may thus reveal important information on the mechanism of each manifestation, as well as the energy conversion process itself. When deducing the initial time of the type III radio bursts from the data of dynamic spectra, we may also obtain the start frequency of each individual type III burst signal. These frequencies provide information on the accelerating region, including the plasma density and the corresponding altitude if the plasma density model is known.

We plot the number of events versus the starting frequencies of the type III burst in Figure 4. We notice that more than 30 events produced type III bursts with a starting frequency of around 750 MHz, and about 10 events showed a starting frequency of 1.1 GHz. According to the dependence of the radio emission frequency on the plasma density, $f(\text{GHz}) = 0.898\sqrt{n_e(10^{10} \text{ cm}^{-3})}$, we realize that these two frequencies correspond to two plasma densities of $7 \times 10^9 \text{ cm}^{-3}$ and $1.5 \times 10^{10} \text{ cm}^{-3}$, respectively. For the given model of the coronal plasma density, for example that by Sittler & Guhathakurta (1999), these two densities suggest that the type III radio bursts were initially excited in the low corona where the energetic electron beams were produced.

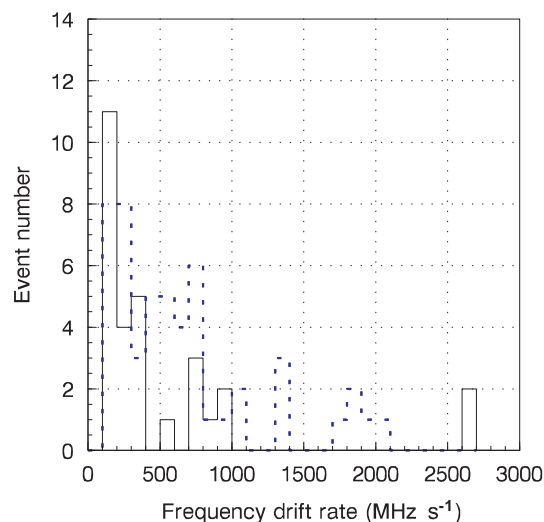


Fig. 5 Numbers of events versus the frequency drifting rates. The solid and dashed histograms represent positive and negative drifting rates, respectively.

Theories and observations indicate that both the CME-driven shock and the electric field in the current sheet are candidates of accelerating electrons responsible for the type III bursts (e.g., see Cane et al. 2002; Lee 2005; Lin et al. 2006). Usually, the CME-driven shock does not form until the CME reaches certain altitudes, generally a few 10^5 km from the surface of the Sun, where the frequencies of radio emissions are lower than 200 MHz (e.g., see Lin et al. 2006 and references therein). Therefore, the electron beams that accounted for the type III bursts investigated in the present work were not produced by the CME-driven shock, but by the electric field inside the current sheets which developed during the eruptions (Forbes & Lin 2000; Lin & Forbes 2000).

When investigating the rate of frequency drift of the type III burst, we recognized many positive drifting bursts that imply the propagation of the electron beams toward the Sun. We carefully measured the drifting rates for all the 395 type III radio bursts, realized that accurate drifting rates could be obtained for 370 out of the 395 events, and found that 210 bursts displayed a positive drifting rate and 160 showed a negative one, which indicates that the electron beams are moving away from the Sun. Figure 5 plots the number of events which were associated with both CMEs and H α flares, versus the frequency drift rate. We have identified a total of 84 such events from the 395 events collected in this work. Four of these 84 events manifested incredibly large drifting rates (> 10 GHz s $^{-1}$), and they are not shown in Figure 5.

It can be seen from the figure that most of the drifting rate, no matter whether negative or positive, occurred in the range from 100 to 200 MHz s $^{-1}$, that the positive drifting rates were basically slower than 1 GHz s $^{-1}$, and that the negative drifting rates dispersed over a wider range extending up to 2 GHz s $^{-1}$. Appearance of both positive and negative frequency drifts further suggests that the electron beams igniting the decimetric type III radio bursts were accelerated in the reconnection region, namely the current sheet.

Before ending this part of the work, we briefly describe the properties of 84 H α flares that were associated with both CMEs and type III radio bursts. From the information provided by SGD and CSGD, we find that 18 flares were SF and SN flares (e.g., see Švestka 1976 for detailed descriptions of the H α flare importance), 21 had an importance of 1, two had an importance of 2, and 36 were 3B

flares. So in the 84 events we studied here, only 33% of them produced SF and SN flares, and most (67%) of them gave rise to major ones (importance ≥ 1).

Further analyses indicate that the CME speeds increase with the importance of the associated flares. Following the practice of Özguc et al. (2003), we use the flare index $Q = IT$ to help specify the flare importance in a more quantitative fashion. Here, I is the quantified flare importance that is related to the conventional one in the way displayed in Table 1, and T is the duration of the $H\alpha$ flare. Using the information we collected for the 84 events that showed associations of CMEs to both flares and type III radio bursts, we are able to calculate Q and investigate how the speed of CMEs is related to Q . We listed the average values of these parameters in Table 1 for the 84 events according to their $H\alpha$ importance. The information revealed by such arrangement shows apparent correlation of the CME speeds to the importance of the associated flares as expected (e.g., see Lin 2004; Yashiro et al. 2005).

Table 1 Various Parameters of $H\alpha$ Flares and the Associated CMEs

Flare Importance	Event Number	I	T	Q	CME Speed (km s ⁻¹)
SN, SF	18	0.5	121	61	684
1N, 1F	21	1.0	97	97	967
2N	2	2.0	76	152	1218
2B	7	2.5	94	235	1664
3B	36	3.0	142	426	2103

4 SUMMARY AND DISCUSSION

We statistically studied 395 solar eruptive events that produced type III radio bursts. Among these events, 150 type III bursts showed correlation to the $H\alpha$ flares and 187 bursts were associated with CMEs if only the relationship among them with respect to time was considered. To improve the accuracy and reliability of the deduced correlation, we considered the locations of these flares and CMEs simultaneously, as another two crucial factors governing the correlation. We then found that 84 out of 395 type III radio bursts were associated with both flares and CMEs, and that 53 flares took place before CMEs and 31 after CMEs.

Our main results are summarized as follows:

First of all, the correlation of the decimetric type III radio burst to both $H\alpha$ flares and CMEs is about 21%. Most of them occurred about 5 min before the associated CMEs. The correlation of decimetric type III bursts to CMEs is apparently lower than that of type II radio bursts to CMEs, which reaches 80% (e.g., see Munro et al. 1979; Chernov 1997; Shanmugaraju et al. 2003, Ma 2005).

We compared the results of Ma et al. (2006), which investigated a similar correlation of type III radio bursts in the microwave band, and found that the correlation of the microwave type III bursts (33%) is slightly higher than that of the decimetric type III radio bursts. Consulting previous works on the correlation of flares to CMEs, and the related energy conversion process, we realize that the association of type III radio bursts to both flares and CMEs is governed by the energetics of the eruptive process: the more energetic the eruption is, the better the correlation is.

Second, the $H\alpha$ flares associated with CMEs are all gradual flares, of which 82% erupt before the CMEs, with the occurrence being within the first 33 min on average. Only 18% of the flares occurred after the CMEs, with the occurrence being within the last 29 min on average.

Third, the start frequencies of most type III radio bursts associated with CMEs are about 750 MHz, and the corresponding frequency drifting rate ranges from 100 to 200 MHz s⁻¹.

Fourth, many positive drifting rates of the type III burst were observed, indicating that the energetic electron beams were propagating towards the Sun. The high start frequency (750 MHz) of the

type III burst suggests that the accelerating region of these electrons is located in the lower corona, say ≤ 0.1 solar radius from the solar surface. According to Lin et al. (2006), the reconnecting current sheet which developed in the eruptive process is most likely the unique acceleration site at such an altitude in the solar atmosphere.

Finally, as expected, the flares and the CMEs associated with the type III bursts studied in the present work show good correlations to one another: the faster the CME is, the larger the associated flare is. Related to this result is the poor correlation of the type III radio burst to the CME without being associated with a flare. Understanding the physics behind this result is not difficult. It has long been known that type III radio bursts are more likely to be associated with flares than CMEs (e.g., see Švestka 1976). An eruptive process that does not manifest an apparent flare phenomenon is suggestive of weak, or even a lack of, magnetic reconnection (see discussions in Lin 2004 and Bao et al. 2007, and references therein), and we can hardly expect the production of energetic particles in this kind of eruption. The reason for this is two-fold. First of all, the weak reconnection means a weak electric field induced in the reconnection region and a slow energy conversion process. In this case, heating and kinetic energy converted from the magnetic field are not enough to produce major flares and energetic particles accounting for type III radio bursts. Second, the CME-driven fast mode shock is another candidate for producing energetic particles. However, CMEs that are not associated with flares are usually slow and cannot invoke the fast mode shock. So, no energetic particles could be created in this case either. Therefore, both cases indicate that energetic particles cannot be produced in an eruption that develops the CME without an associated flare, and a poor correlation of the type III radio burst to the CME alone is thus expected.

Acknowledgements This work was supported by the Ministry of Science and Technology of China under the 973 Program grants 2006CB806301 and 2006CB806303, by the National Natural Science Foundation of China (Grant Nos. 10473020, 10333030 and 10873030), and by the Chinese Academy of Sciences under the grant KJCX2-YW-T04 to YNAO. JL acknowledges NASA grant NNX07AL72G for supporting his visit to CfA.

References

- Aschwanden M. J. 2002, Particle acceleration and kinematics in solar flares A Synthesis of Recent Observations and Theoretical Concepts (Invited Review), eds. by Ma. J. Aschwanden, & L. Martin, Advanced technology Center, palo Alto, California, U.S.A. Reprinted from SPACE SCIENCE REVIEWS, 101, 1 (Dordrecht: Kluwer Academic Publishers)
- Bao, X., Zhang, H., Lin, J., & Stenborg, G. A. 2007, A&A, 463, 321
- Bastian, T. S., Benz, A. O., & Gary, D. E. 1998, ARA&A, 36, 131
- Cane, H. V., Erickson, W. C., & Prestage, N. P. 2002, J. Geophys. Res. (Space Physics), 107, 1315
- Cecatto, J. R., Fernandes, F. C. R., Soares, A. C., Madsen, F. R. H., Andrade, M. C., Sych, R. A., & Sawant, H. S. 2004, 35th COSPAR Scientific Assembly, 35, 3123
- Chernov, G. P. 1997, Astronomy Letters, 23, 827
- Dulk, G. A., Leblanc, Y., Bastian, T. S., & Bougeret, J.-L. 2000, J. Geophys. Res., 105, 27343
- Forbes, T. G., & Lin, J. 2000, Journal of Atmospheric and Solar-Terrestrial Physics, 62, 1499
- Ginzburg, V. L., & Zhelezniakov, V. V. 1958, Soviet Astronomy, 2, 653
- Gopalswamy, N. 2004, in The Sun and The Heliosphere Intergrated System, eds. G. Poletto, & S. T. Suess (Dordrecht: Kluwer), 201
- Jackson, B. V., Sheridan, K. V., Dulk, G. A., & McLean, D. J. 1978, Proceedings of the Astronomical Society of Australia, 3, 241
- Klassen, A., Pohjolainen, S., & Klein, K.-L. 2003, Sol. Phys., 218, 197
- Lee, M. A. 2005, ApJS, 158, 38

- Lin, J. 2004, *Sol. Phys.*, 219, 169
- Lin, J., & Forbes, T. G. 2000, *J. Geophys. Res.*, 105, 2375
- Lin, J., Salvatore, M., & Angelos, V. 2006, *ApJ*, 649, 1110
- Lin, R. P., & Anderson, K. A. 1973, *BAAS*, 5, 275
- Ma, Y. 2005, *Astronomical Research and Technology*, 2, 99
- Ma, Y., Wang, D. Y., & Yan, Y. H. 2006, *Astronomical Research and Technology*, 3, 321
- Maia, D., Pick, M., Kerdraon, A., Howard, R., Brueckner, G. E., Michels, D. J., Paswaters, S., Schwenn, R., Lamy, P., Llebaria, A., Simnett, G., & Aurass, H. 1998, *Sol. Phys.*, 181, 121
- Michalek, G., Gopalswamy, N., Reiner, M., et al. 2001, *AGU Spring Meeting Abstracts*, 22
- Michalek, G., & Zaczkowski, R. 2002, in *Solar variability from core to outer frontiers, The 10th European Solar Physics Meeting*, ed. A. Wilson, ESA SP-506, 1, 185
- Munro, R. H., Gosling, J. T., Hildner, E., MacQueen, R. M., Poland, A. I., & Ross, C. L. 1979, *Sol. Phys.*, 61, 201
- Özgüç, A., Ataç, T., & Rybak, J. 2003, in *Solar variability as an input to the Earth's environment, International Solar Cycle Studies (ISCS) Symposium*, ed. A. Wilson, ESA SP-535, 141
- Reiner, M. J., Karlický, M., Jiříčka, K., Aurass, H., Mann, G., & Kaiser, M. L. 2000, *ApJ*, 530, 1049
- Reiner, M. J., Klein, K.-L., Karlický, M., Jiříčka, K., Klassen, A., Kaiser, M. L., & Bougeret, J.-L. 2008, *Sol. Phys.*, 249, 337
- Shanmugaraju, A., Moon, Y. J., Dryer, M., & Umapathy, S. 2003, *Sol. Phys.*, 217, 301
- Sheeley, N. R., Jr., Howard, R. A., Michels, D. J., Robinson, R. D., Koomen, M. J., & Stewart, R. T. 1984, *ApJ*, 279, 839
- Sittler, E. C., Jr., & Guhathakurta, M. 1999, *ApJ*, 523, 812
- Švestka, Z. 1976, *Solar Flare* (Dordrecht: Reidel)
- Wang, J., Zhou, G., Wen, Y., Zhang, Y., Wang, H., Deng, Y., Zhang, J., & Harra, L. K. 2006, *ChJAA (Chin. J. Astron. Astrophys.)*, 6, 247
- Yan, Y., Pick, M., Wang, M., Krucker, S., & Vourlidas, A. 2006, *Sol. Phys.*, 239, 277
- Yashiro, S., Gopalswamy, N., Akiyama, S., Michalek, G., & Howard, R. A. 2005, *J. Geophys. Res. (Space Physics)*, 110, 12